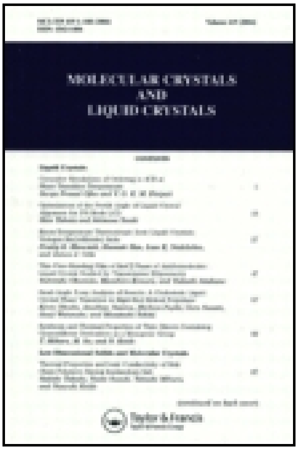

Molecular Crystals and Liquid Crystals

Publication details, including instructions for authors and subscription information:
http://www.tandfonline.com/loi/gmcl16

A Molecular Dynamics Simulation of an ODIC Phase

M. Yvinec [a]

[a] Département de Recherches Physiques, Université Pierre et Marie Curie, 4 Place Jussieu, 75230 Paris CEDEX 05, France

Version of record first published: 13 Dec 2006.

To cite this article: M. Yvinec (1982): A Molecular Dynamics Simulation of an ODIC Phase, Molecular Crystals and Liquid Crystals, 89:1-4, 359-382

To link to this article: http://dx.doi.org/10.1080/00268948208074490

Mol. Cryst. Liq. Cryst., 1982, Vol. 89, pp. 359–382
0026-8941/82/8904–0359$06.50/0

A Molecular Dynamics Simulation of an ODIC Phase

M. YVINEC

*Département de Recherches Physiques,† Université Pierre et Marie Curie,
4 Place Jussieu, 75230 Paris CEDEX 05 (France)*

(*Received March 10, 1982; in final form April 23, 1982*)

We present here the first results derived from a molecular dynamics simulation of an ODIC phase. The model is a two-dimensional schematization of the sodium cyanide crystal NaCN. Our results are related to the structural aspect of the orientational disorder and the individual rotational dynamics of the molecules. This dynamics involve both large amplitude reorientations and librational excitations. From the computed rotational correlation functions we can deduce a value of about 1 pcs for the relaxation time of the reorientational motions. The librational modes are shown to give rise to a very broad spectrum, its linewidth being essentially due to inhomogeneous broadening effects.

I INTRODUCTION

The initials ODIC (Orientation Disorder In Crystals) form a now widely used abbreviation to name the high temperature plastic phase of some molecular crystals. ODIC phases appear as an interesting intermediate case between liquid and solid state. Indeed, in those phases, the average centers of mass positions still form a regular lattice, while molecular orientations display some degree of disorder. In the recent past years, a large amount of experimental work (see for instance Refs. 1 and 2), including various techniques such as X-ray and neutron scattering, N.M.R., infrared and Raman spectroscopy, picosecond methods, etc. . . . , has been devoted to ODIC crystals. These studies show that the structural disorder is generally related to a complex rotational

---

† L.A. N°71 (C.N.R.S.).

dynamics of the molecules which involves large amplitude reorientations as well as librational excitations around some preferred orientations. Furthermore, the steric hindrance in the crystal implies generally that each instantaneous configuration of the molecular orientations is related to a special pattern of local distortions in the center of mass lattice apart from the high symmetry average structure. Large amplitude reorientations occur only by means of fluctuations of these local distortions and appear thus to be strongly coupled to the low frequency translational lattice phonons. From a theoretical point of view, the usual solid state methods fail to describe the dynamics of ODIC phases since the large amplitude rotational motions do not allow for an harmonic approximation or a perturbation expansion of higher order terms. In this field, the work of K. H. Michel *et al.*[4-6] is an interesting attempt to overcome this difficulty†. Nevertheless, it is still appealing to apply to those disordered phases methods which are borrowed from the liquid state physics. In particular, we felt that computer simulations using molecular dynamics techniques should provide a more clear insight of the complex dynamics in ODIC phases.

To build up a model of ODIC phase, suitable for a molecular dynamics simulation we get ideas from previous works on the high temperature phase of sodium cyanide (NaCN, see Refs. 6–13). This crystal is an inviting example of ODIC crystal since it displays most of the complex features of plastic phases within the simple geometrical framework of a linear dumbbell molecule embedded in a cubic site. Indeed, the high temperature phase (phase I) of sodium cyanide has the fcc rocksalt structure (space group O_h^5, $Z = 1$). The overall cubic symmetry results from the disorder in the orientation of the CN^- dumbbells which align preferrentially along the [1, 0, 0] directions.[7-9]

Ultrasonic,[10] Brillouin[11] and neutron scattering data,[12] provide anomalous dispersion curves for the TA branches showing a strong coupling between the CN^- reorientations and the low frequency acoustic modes. Furthermore, the shear elastic constant, C_{44}, shows a critical softening when the crystal is cooled near the temperature of the transition toward the ordered phase II. The neutron experiments provide no clear evidence for the existence of librational modes,[12] but these modes appear as a broad band (from 50 cm^{-1} up to 250 cm^{-1}) in the low frequency F_{2g} Raman spectra.[13]

---

† In this work, the crystal Hamiltonian is expanded in terms of small translational displacements of the centers of mass and on a set of symmetry adapted functions of the angular coordinates. The formalism of the Mori projection method is then used to derive coupled dynamics equations for the relevant secular variables of the problem.

A molecular dynamics simulation of the phase I of NaCN has recently been performed by M. L. Klein and I. R. McDonald.[14] These authors built up a small sample of 32 formular units, and obtained computed neutron cross sections which show the critical softening of transverse acoustic phonons near the I–II phase transition. We, here, are merely interested in the fundamental mechanisms of the librational and reorientational dynamics of such a plastic phase and we decided to build up a two dimensional model which is to be regarded only as an idealization of the NaCN case. A two dimensional model makes the computational work faster since each CN^- has only one rotational degree of freedom, this allows to simulate a larger system which should provide a more clear insight of the collective dynamical behavior of the CN^- dumbbells. Indeed, in the nearest future we are interested in the study of the reorientation translation coupling and in the presence of a collective reorientational dynamics; however, for the moment, we present here the first results derived from this molecular dynamics simulation which only concern the structural aspect of the orientational disorder and the individual rotational dynamics of the molecules in the crystal. These results seem nevertheless interesting as they clearly confirm some general ideas which have been suggested in the analysis of experimental data.[13]

The next part (part II) is devoted to describe the general features of the simulated system, the interaction model and a few technical aspects of the computer simulation. In part III, we present the first results derived from this simulation. Some structural aspects of the orientational disorder are first described, then we show the general behavior of the individual rotational dynamics which include librations and reorientations. More quantitative data, such as the inhomogeneous dispersion of librational frequencies and the relaxation time of orientational potential wells are then derived from the analysis of the computed rotational self-correlation functions.

II THE MODEL

As mentioned in the introduction, we present here the computer simulation of a fictuous two dimensional molecular crystal which only has some common features with the three dimensional NaCN crystal, such that it can be regarded as a schematization of this real crystal.

The simulated system can be described as a two dimensional ionic compound $A^+ XY^-$. The negative ions XY^- are rigid symmetric dumbbells of length d which are bound to lie in the two dimensional plane of the system. Thus the model implies only five degrees of freedom per formular unit ($A^+ XY^-$), which are described by

- the two translational coordinates of the A^+ ions
- the two translational coordinates of the center of mass of the XY^- dumbbell
- one angular coordinate describing the orientation of the dumbbell XY^-.

The evolution of this system is assumed to be driven by a simple set of pair interactions which, besides Coulomb forces, includes a repulsive interaction between each end of the XY^- dumbbells and the surrounding A^+ ions. In this model the XY^- dumbbell is assumed to have a head-to-tail symmetry: the repulsive interaction potential between A^+ ions and each end of the dumbbell is given the exponential forms $\lambda e^{-r/r_0}$ with only two parameters λ and r_0, and, for the Coulomb interactions, the dumbbell XY^- is considered as a simple monopole with an electric charge $-|q|$ located at the center of mass, the A^+ ions having the charge $+|q|$. The higher moments (essentially quadrupolar) of the charge distributions are simply neglected so that the electrostatic part of the potential is independent of the dumbbells orientation. At last, it is to be noted that, for the moment, this model includes no direct coupling between the orientations of neighboring XY^- ions.

The numerical values assumed for the various parameters of this model are listed in Table I. These are only reasonable values which do not correspond to any real physical system. For instance, we choose for the electrostatic constant $q^2/4\pi\epsilon_0$ the value corresponding to an

TABLE I

Numerical values of the different parameters used as input data in the computer simulation.

Coulomb interaction	$q_{A^+} = -q_{XY^-} = 1.6\ 10^{-19}$ C $\frac{q^2}{4\pi\epsilon_0} = 14.42$ eV Å^{-1}
Repulsive interaction $\lambda e^{-r/r_0}$	$\lambda = 459.5$ eV $r_0 = 0.358$ Å
Length of the dumbbell	$d = 0.6$ Å
Kinetic parameters:	
—masses	$M_{A^+} = M_{XY^-} = 25$ u.m.a.
—inertial moment of the dumbbell	$I = 2\,M_{XY^-}\frac{d^2}{4}$

electronic charge, the parameters λ and r_0 were given the values quoted by Born and Huang[15] for NaCl. In addition we choose the length d of the dumbbell to get both a reasonable lattice parameter and a reorientational potential barrier of about 1000 K if a square lattice configuration is assumed for the center of mass (cf. below). At last, we choose the kinetic parameters: the mass of A^+ and XY^- were chosen to equal and the inertial moment was also chosen independently so that the bottom well librational frequency falls in the frequency range of the zone boundary acoustic phonons.

The above described forces lead to a low temperature structure which we had to discover. A possible technique to look for this structure would be the use of the Rahman-Christiansen-Parinello method[16] which allows through a molecular dynamics calculation to alter both the shape and the volume of the periodically repeated original sample and to find the stable configuration of this system. Not knowing the possibility of this method at the beginning of our work, we instead used a classical trial and error method which leads to a rather satisfactory result.

In a first step we assume a square lattice configuration for the centers of mass (Figure 1a), with all the dumbbells aligned along the [1, 0] direction and look for an energy minimum with respect to the lattice parameter a_0 which is found equal to 3.88 Å. (Note that in the square lattice configuration the dumbbells have two equivalent preferred orientations [1, 0] and [0, 1] and that, in the absence of direct coupling be-

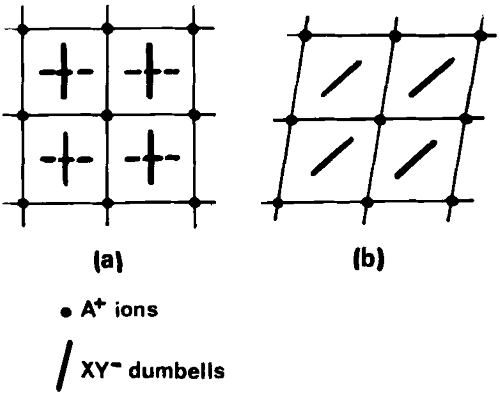

FIGURE 1 Two possible structures candidates for the stable low temperature ordered configuration of the simulated $A^+ XY^-$ system. (a) the square lattice configuration of the centers of mass. In this configuration, the XY^- dumbbells have two equivalent preferred orientations [1, 0] and [0, 1] which are drawn in respectively broken and full lines. (b) the ferroelastic distorted structure.

tween the dumbbells orientations, a disordered structure where the dumbbells point at random in either of those two directions leads to the same energy). We then tested the dynamical stability of the obtained configuration by computing the corresponding harmonic phonons dispersion curves. As could be expected, this structure was found to be Jahn Teller unstable, and this calculation revealed an imaginary transverse acoustic phonon branch (cf. Figure 2). This indicates a tendency for a shear ferroelastic deformation which elongates one diagonal ([1, 1] for example) at the expense of the other one ([1, $\bar{1}$]). We thus looked for an energy minimum for a rectangular centered $2d$ lattice, minimizing for both the lattice parameters a_1 of the corresponding Bravais lattice and the angle α between its two basis vectors, the dumbbells being aligned along the long diagonal of the primitive cell. This led to a value $a_1 \approx a_0$ and to $\alpha = 82$, a structure that we found to be stable against the harmonic vibrations, the dispersion curves showing no sign of anomalous softening of any phonon branch (cf. Figures 1b and 2b).

This method has presumably not given the real ground state of the system and it is quite possible that the actual low temperature structure is a more complex one with many formular unit $A^+ XY^-$ per unit cell as it is the case for most of the real $3d$ plastic crystals. Nevertheless, the study of the presently known cases shows that in these complex structures, the local environment of each molecule and its relative orientations with respect to this environment differ only slightly from one molecule to the other†. We can thus safely state that we have at least obtained the local features of the ground state structure, a statement which will be confirmed in section III by the study of the local structure of the simulated plastic phase (cf. Figure 3).

Let us now make precise some technical aspects of the computer simulation. The infinite crystal was simulated through the periodic repetition of an original square sample of 10 × 10 unit cells. As initial conditions we chose the configuration of the square centers of mass lattice with the XY^- dumbbell aligned at random along either one of the two preferred orientations [1, 0] and [0, 1]. Each degree of freedom was assigned a random initial velocity according to a Maxwellian distribution corresponding to the chosen temperature T_0. The time evolution of the system was then computed through the usual algorithm of Verlet[18] with a time step of 10^{-14} s, chosen to be approximately one

---

† The best-known exception to this rule is the case of phase II of CH_4.[17] This exception can be easily explained by the weakness of the octupole–octupole interaction which favors the James and Keenan phase.

tenth of the shortest characteristic evolution time of the system (the highest optical frequency was estimated from the dispersion curve in Figure 2 to be slightly under 300 cm^{-1}). At each step, the contribution to the long range Coulomb interaction arising from the periodically repeated images of the original sample were summed up via the Ewald method[19] adapted to a two dimensional problem. At last, we computed

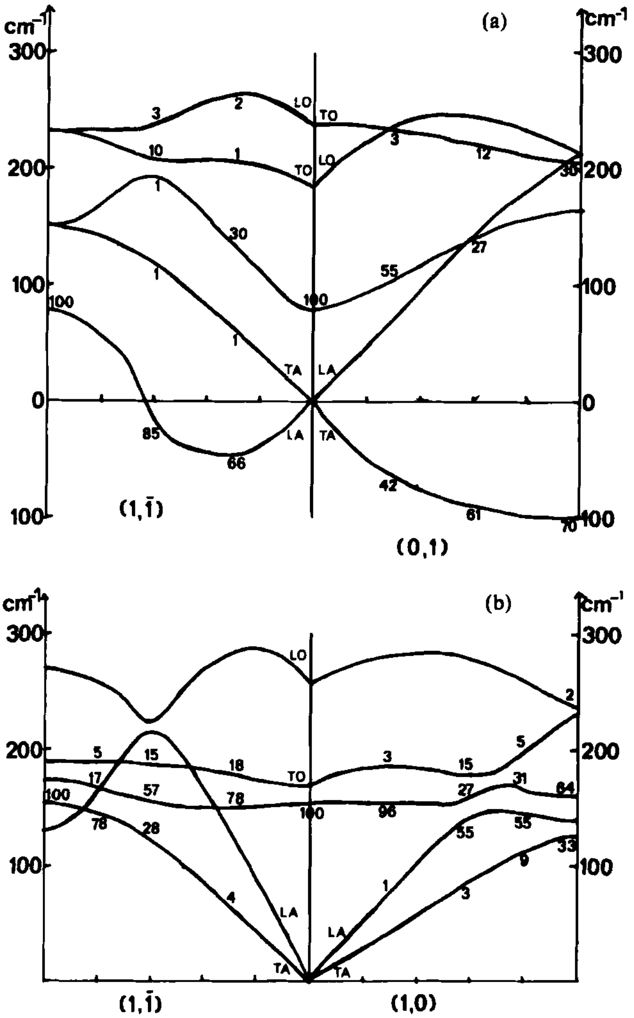

FIGURE 2 Phonon dispersion curves. (a) for a square ordered structure with the dumbbell XY$^-$ aligned along the x axis. The unstable imaginary acoustic branches are represented through the dispersion curves—$\sqrt{|\omega^2|}$ and appear thus in the negative frequency range. (b) for an ordered ferro-elastic distorted structure, the numbers along the curves refer to the percentage of librational character of the mode.

at each step the total energy of the system to check the accuracy of the integration method. The total energy of the system showed no shift over the full integration time and its fluctuations remained less than 5% of the kinetic energy fluctuations.

III RESULTS

A first attempt showed us that at the kinetic temperature 200 K the system relaxed towards an ordered structure of "herring bone" type so we decided to raise the temperature up to 300 K where we actually got a disordered plastic phase (see Figure 3). The results presented here are derived from two independent numerical experiences, each of which running over 2560 steps which means a total evolution time of 25 pcs. In the first part, we give some general features of the structural disorder, though the detailed structural analysis of the obtained plastic phase will be the subject of a forthcoming paper. Then, we present the rotational dynamics of the dumbbells in its individual aspect. This dynamics can be qualitatively understood through the time variation of the angular coordinates $\theta(t)$. More quantitative informations, such as the librational lifetime, can be derived from the computation of rotational self-correlation functions $\langle f[\theta(t)]f[\theta(0)]\rangle$ for different functions f of the angle $\theta(t)$. At last, we show that in this plastic phase, the large spectral linewidth of the librational modes, as it can be observed through e.g. Raman or neutron spectroscopy, arises essentially from the spatial inhomogeneity in the instantaneous configurations of the different orientational potential wells throughout the sample.

A Structural aspect of the orientational disorder

It is first interesting to look at the ordered "herring bone" configuration obtained at the kinetic temperature 200 K (Figure 3a). This structure appears as a succession of domains with right or left ferroelastic distorted structure. Of course, the detailed succession of these domains is strongly related to the size of the original sample and to the periodic boundary conditions, but each domain is clearly reminiscent of the ordered ferroelastic distorted structure described in part II as a possible candidate for the low temperature ground state. In particular, the angular distortion, averaged over the hundred cells of the sample is about 83°, which is very close to the angular value $\alpha = 82°$ obtained by minimizing the potential energy of the ferroelastic configuration.

Let us now come to the disordered phase obtained at 300 K. On the

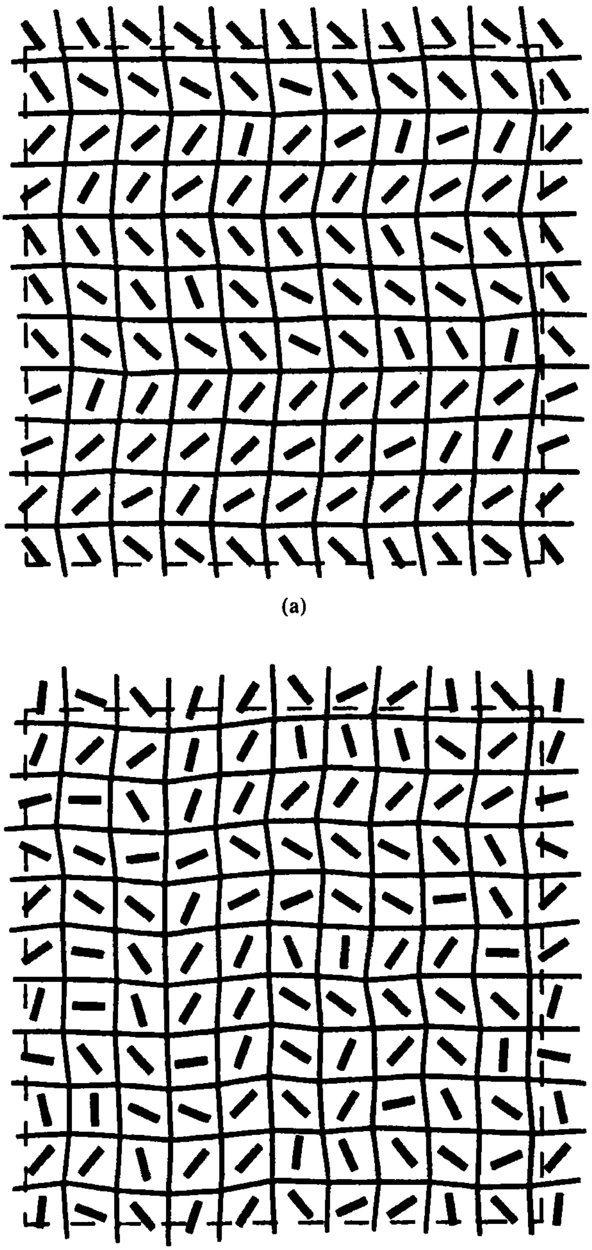

FIGURE 3 Instantaneous configurations of the simulated sample. (a) $T = 200$ K: ordered "herring bone" phase. (b) $T = 300$ K: disordered phase.

one hand, Figure 3 shows an instantaneous configuration of the system. In this configuration, most of the A^+ cages appear to be distorted, with a clear tendency to spatial correlations of these distortions in either ferro or antiferro local patterns. On the other hand, the structural properties of this disordered system can be described through the time average values, or better, the probability distribution functions (pdf) of some relevant variables such as the centers of mass coordinates and the dumbbells orientations. This analysis confirms the average square symmetry (C_{4v}) of the high temperature phase. For instance the average centers of mass positions are actually the initial square positions. The probability density function (pdf) $P(\theta)$ of the dumbbell orientations is given in Figure 4. This function clearly exhibits this symmetry with the two preferred orientations $\theta = \pi/4$ ([1, 1]) and $\theta = 3\pi/4$ ([1, $\bar{1}$]) for the dumbbells. To check this result we have analyzed $P(\theta)$ in a Fourier series

$$P(\theta) = \frac{1}{2\pi}\left[1 + \sum_{n}^{\infty} (a_n \cos n\theta + b_n \sin n\theta)\right] \qquad \text{(III.1)}$$

The result of this analysis is given in Table II and shows that, within the limit of our numerical accuracy, the only non zero coefficients are a_{4p}, as it is to be expected for such a symmetry. Figure 4 and Table II also give the orientational pdf $P_1(\theta)$ for a system of two harmonic oscillators, librating at 300 K with a frequency $\omega = 120\ \text{cm}^{-1}$ around the two equilibrium positions $\theta = \pi/4$ and $\theta = 3\pi/4$. The difference between $P(\theta)$ and $P_1(\theta)$ arises from two effects:

a) in each instantaneous configuration of the simulated system the equilibrium orientations of each individual molecule can differ slightly from $\theta = \pi/4$ or $3\pi/4$.

b) as we shall see in the following (part III B), reorientations processes take place with a finite time, allowing a finite probability to find the angular coordinate θ out of the equilibrium positions.

In conclusion, we can say that the simulated system actually presents an average square (C_{4v}) symmetry. However this symmetry is only a mean property which arises from the spatio-temporal averaging of the fluctuations of local distortions. These local distortions are reminiscent of the local features of the low temperature structure and the local instantaneous aspects of the simulated system show no evidence of the average C_{4v} symmetry of the whole system. In other words, the simulated plastic phase is, in fact, a rather unusual system where the relevant pdf are not Gaussian like so that the mean value of orientational and positional coordinates are in fact quite different from their most probable values. This aspect of the simulated system appears quite obviously if we consider the following fact: for each configuration encountered in the molecular dynamics run and each dumbbell in the sample we can compute the orientational part $V(\theta)$ of the potential energy, a function of the angular coordinate θ. On the one hand the pdf $P(\theta)$ (which has been computed from the dynamical data of the molecular dynamics run) is very close to the spatio temporal average value $\langle e^{-\beta V(\theta)}\rangle$ of the maxwellian distribution associated with each potential $V(\theta)$. On the other hand, we can compute the mean orientational potential $\langle V(\theta)\rangle$ experienced by the dumbbells. The mean value $\langle V(\theta)\rangle$ of the orientational potential reflects only the average structure and looks very much like the orientational potential arising from the average

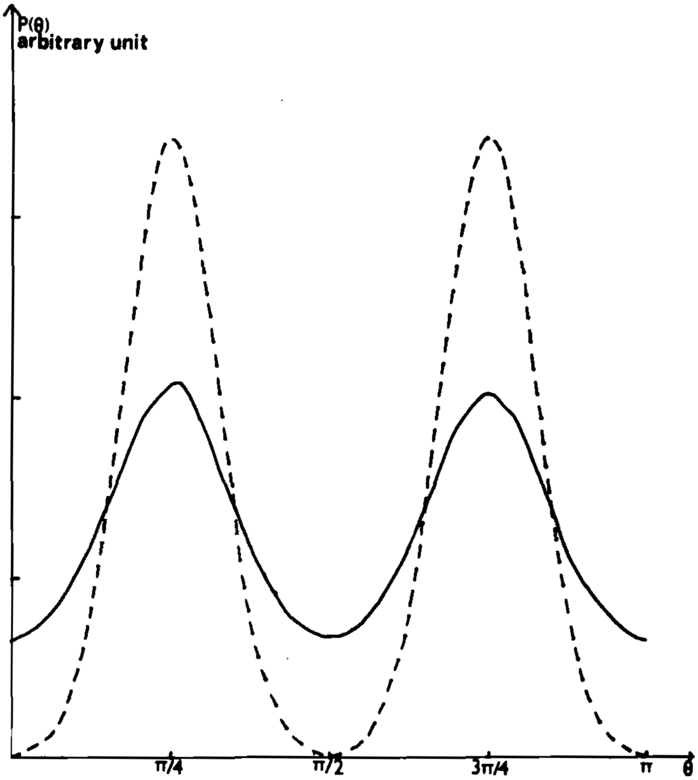

FIGURE 4 Probability density function $P(\theta)$. (a) *full line*: results from the 300 K molecular dynamics simulation. (b) *broken line*: system of two identical harmonic potential wells around the directions $\theta = \pi/4$ and $\theta = 3\pi/4$ at 300 K with a librational frequency of 120 cm^{-1}.

TABLE II

Coefficient of the Fourier development

$$\frac{1}{2\pi}\left[1+\sum_{n}(a_n \cos n\theta = b_n \sin \theta)\right]$$

- for $P(\theta)$ the pdf computed from the computer simulation data at 300 K.
- for $P'(\theta)$ orientational pdf for a model of two harmonic potential wells (with frequency of 120 cm^{-1}) at 300 K.

	$P(\theta)$	$P'(\theta)$		$P(\theta)$	$P'(\theta)$
a_1	0.008	—	b_1	0.001	—
a_2	−0.004	—	b_2	0.010	—
a_3	−0.005	—	b_3	0.007	—
a_4	−0.526	−1.303	b_4	0.003	—
a_5	0.001	—	b_5	−0.010	—
a_6	0.003	—	b_6	−0.004	—
a_7	0.000	—	b_7	0.000	—
a_8	+0.069	+0.357	b_8	0.002	—
a_9	0.001	—	b_9	0.009	—
a_{10}	−0.002	—	b_{10}	0.000	—
a_{11}	0.000	—	b_{11}	0.000	—
a_{12}	−0.010	−0.043	b_{12}	−0.004	—
a_{13}	0.004	—	b_{13}	−0.007	—
a_{14}	−0.003	—	b_{14}	0.000	—
a_{15}	0.001	—	b_{15}	0.005	—
a_{16}	−0.002	0.001	b_{16}	0.003	—

square configuration of the centers of mass lattice. This mean potential $\langle V(\theta)\rangle$ would lead to a maxwellian pdf $e^{-\beta\langle V(\theta)\rangle}$ which is quite opposite to the actual $p(\theta)$ and would give as preferred orientations the two directions $\theta = 0°$ ([1, 0]) and $\theta = \pi/2$ ([0, 1]).

B The rotational dynamics of individual molecules

a) A qualitative description of the rotational dynamics of the individual molecules is given by drawing the time evolution of the angular coordinate $\theta(t)$ for a few dumbbells in the sample (cf. Figure 5). For each dumbbell, we find a sequence of time intervals during which the dumbbell has a librational motion (these time intervals will be called shortly librational intervals in the following) interrupted by large amplitude reorientations. This behavior is very similar to the two steps stochastic model introduced by Larsson,[20] the main difference coming from the fact that, in our system, the librations take only place around one of the two preferred orientations [1, 1] and $[1, \bar{1}]$, in complete agreement with the shape of the pdf $P(\theta)$.

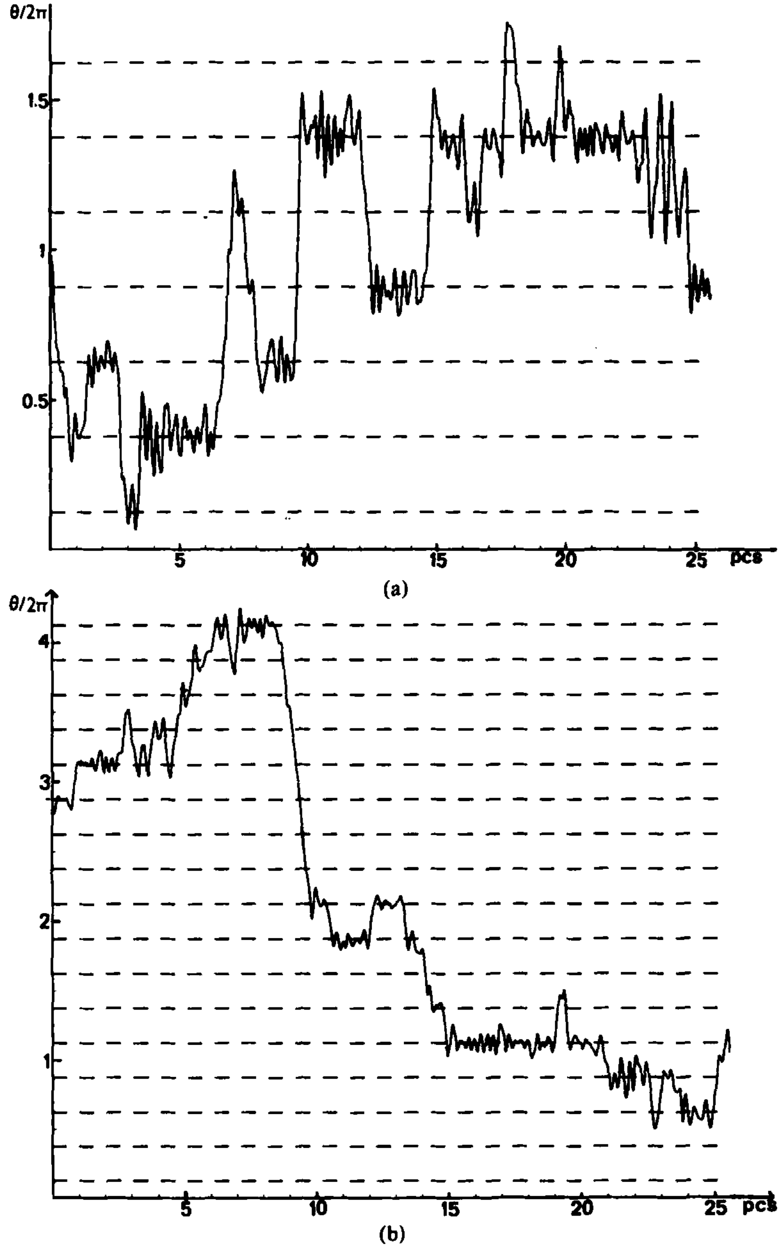

FIGURE 5 (a) and (b) Rotational motion of a XY⁻ dumbbell in the course of a 2560 steps (25 pcs) molecular dynamics run. *Y axis*: angular coordinate θ of the dumbbell modulo 2π. The *broken lines* show the positions of the preferred orientations.

b) Let us now derive more quantitative informations through the analysis of rotational self-correlation functions

$$F(t) = \frac{\langle f[\theta(t)]\, f[\theta(0)]\rangle}{\langle f[\theta(0)]\, f[\theta(0)]\rangle} \tag{III.2}$$

or, of the associated spectral density

$$F(\omega) = \frac{1}{2\pi}\int_0^{\infty} F(t)\cos\omega t\, dt \tag{III.3}$$

which can be computed for any function f of the angular coordinate θ of a dumbbell†. The behavior of the time correlation $F(t)$ and the line-shape of its spectral density $F(\omega)$ largely depend upon the chosen test function f and, before describing your results we need to make this point a little more precise (see also Ref. 21). For each instantaneous angular position $\theta(t)$ of a dumbbell, we can define $\theta_s(t)$ as the angular coordinate of the preferred orientation which is the nearest from $\theta(t)$, and write

$$\theta(t) = \theta_s(t) + \Delta\theta(t) \tag{III.5}$$

with

$$\Delta\theta(t) = \theta(t) - \theta_s(t)$$

whence

$$f[\theta(t)] = f[\theta_s(t)] + f'[\theta_s(t)]\,\Delta\theta(t) + \ldots. \tag{III.6}$$

The variable $\theta_s(t)$ takes only a finite set of possible values and can be considered as a "pseudo spin" variable associated with the rotational

---

† In Eq. (III.2), the symbol ⟨ ⟩ stands for a thermal average which, in an ergodic system, is equivalent to the time average

$$F(t) = \lim_{T\to\infty}\frac{1}{T}\int_0^T f[\theta(\tau)]\, f[\theta(t+\tau)]\, d\tau \tag{III.4}$$

In our calculation, $F(t)$ was approximated by, first, computing for each dumbbell the average (III.4) over the complete duration of the molecular dynamics run and then, performing an average over the hundred dumbbells of the sample. The spectral density $F(\omega)$ was finally obtained through a Fast Fourier Transform routine. Our simulation, due to its finite duration, provides the correlation function $F(t)$, with a sufficient statistical accuracy, over a limited time of about 5 pcs, which, owing to the assumed time reversal symmetry of $F(t)$, implies a frequency resolution of about 3 cm^{-1} for the spectral density $F(\omega)$.

dynamics of dumbbells. This pseudo spin variable remains constant during the librational intervals and only changes during the large amplitude reorientations of the dumbbell from one potential well to another. In other words, the dynamics of the pseudo spin $\theta_s(t)$ reflects only the reorientational dynamics of dumbbells, while the librational aspect is included in the fluctuations of the difference $\Delta\theta(t)$.

Depending on the relative values of the test function $f(\theta_s)$ and of its derivative $f'(\theta_s)$ for all the possible values of the pseudo spin, we can have one of the two following cases:

(1) the correlation $F(t)$ arises essentially from the first term of Eq. (III.6) which is numerically dominant: the behavior of $F(t)$ then reflects only the reorientational dynamics of the dumbbells. This occurs, in particular, when the test function $f(\theta_s)$ happens to have an extremum for the preferred orientations (in which case $f'(\theta_s) = 0$).

(2) the second term (III.6) is the dominant one: this occurs essentially when $f(\theta_s)$ vanishes for each possible potential well. Then the correlation function reflects the librational part of the dumbbell dynamics.

In our two dimensional model, the natural test functions are the trigonometric functions cos $n\theta$, sin $n\theta$ which are just the analogue of the symmetry adapted functions introduced in Ref. 22 for two and three dimensional molecules and chosen as secular variables in the theory of K. H. Michel.[3-5]

In Figures 6 and 7, we show the spectral density $S_2(\omega)$, $S_1(\omega)$, and $C_2(\omega)$ of the following correlation functions:

$$S_2(t) = \frac{\langle \sin 2\theta(t) \sin 2\theta(0) \rangle}{\langle \sin 2\theta(0) \sin 2\theta(0) \rangle} \tag{III.7a}$$

$$S_1(t) = \frac{\langle \sin \theta(t) \sin \theta(0) \rangle}{\langle \sin \theta(0) \sin \theta(0) \rangle} \tag{III.7b}$$

$$C_2(t) = \frac{\langle \cos 2\theta(t) \cos 2\theta(0) \rangle}{\langle \cos 2\theta(0) \cos 2\theta(0) \rangle} \tag{III.7c}$$

The functions sin 2θ happens to be extremum for the preferred orientations [1, 1] and [1, $\bar{1}$] so that $S_2(t)$ is completely insensitive to the small amplitude librations around these directions. The spectral density $S_2(\omega)$ (Figure 6) is thus characteristic of the reorientational dynamics. It appears like a relaxational central peak with a HWHM of about 8

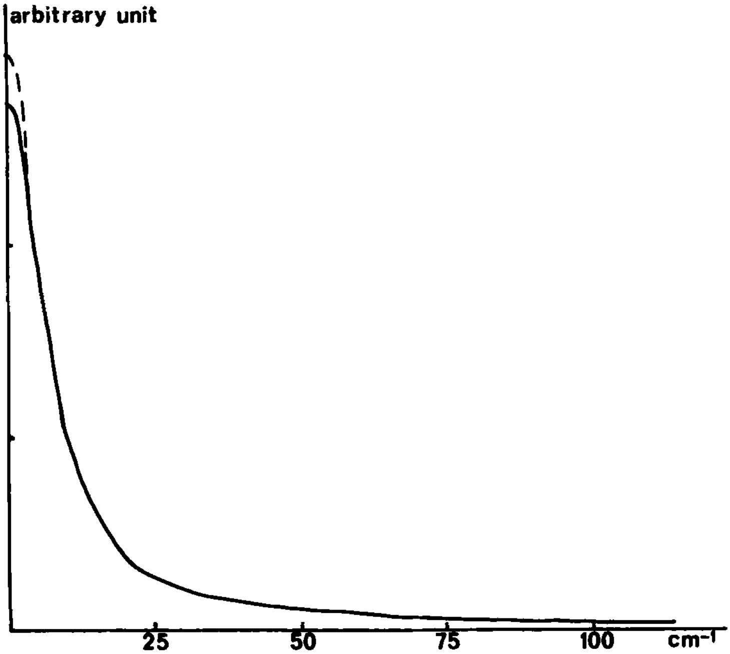

FIGURE 6 Spectral density of two rotational self-correlation functions.

a) *full line*: $S_2(\omega) = TF_\omega \dfrac{\langle \sin 2\theta(t) \sin 2\theta(0)\rangle}{\langle \sin 2\theta(0) \sin 2\theta(0)\rangle}$

b) *broken line*: $S_1(\omega) = TF_\omega \dfrac{\langle \sin \theta(t) \sin \theta(0)\rangle}{\langle \sin \theta(0) \sin \theta(0)\rangle}$

cm^{-1} † and a decaying tail extending up to 50 cm^{-1}. On the other hand, the function cos 2θ vanishes for the preferred orientations and the correlation function $C_2(t)$ actually reflects the librational motion. Its spectral density (Figure 7) exhibits a broad librational band extending from 50 cm^{-1} up to 200 cm^{-1}. A priori, as the function sin θ is such that $|f'(\theta_s)/f(\theta_s)| = 1$ for each preferred orientation, the spectral density could reflect both the librational and reorientational dynamics. In fact, the low frequency reorientational central peak is dominant and just masks completely the librational part so that $S_1(\omega)$ (Figure 6) is very similar to $S_2(\omega)$.

---

† It is to be recalled that this spectral linewidth reflects both, the actual relaxation time of $S_2(t)$ and the spectral resolution (of 3 cm^{-1}) of our calculation.

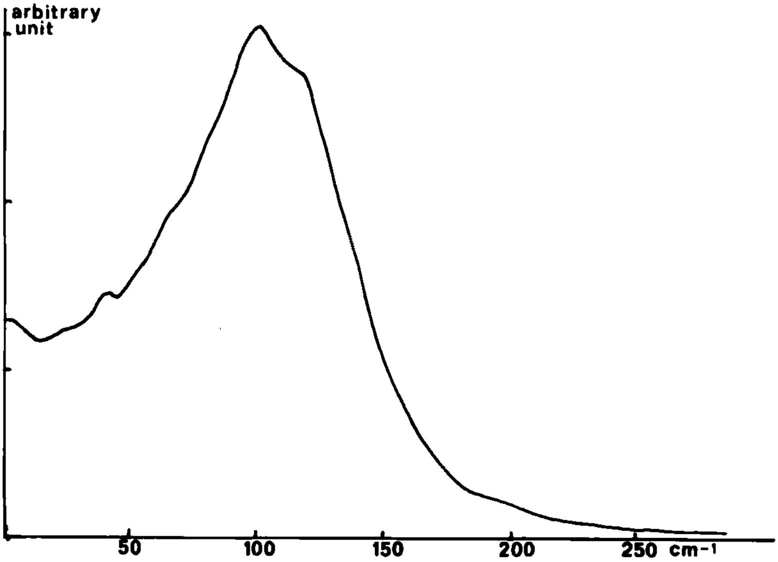

FIGURE 7 Spectral density $C_2(\omega)$ of the rotational correlation function.

$$C_2(\omega) = TF_\omega \frac{\langle \cos 2\theta(0) \cos 2\theta(t) \rangle}{\langle \cos 2\theta(0) \cos 2\theta(0) \rangle}$$

c) Reorientational dynamics. Lifetime of the librational intervals. We have shown above that the spectral densities $S_2(\omega)$ and $S_1(\omega)$ are mostly reorientational. However, to study the reorientational dynamics of the dumbbells it is even simpler to compute the correlations and spectral densities of functions of the pseudo spin variable:

$$S_{2s}(\omega) = \mathrm{FFT}[S_{2s}(t)] \quad S_{2s}(t) = \frac{\langle \sin 2\theta_s(t) \sin 2\theta_s(0) \rangle}{\langle \sin 2\theta_s(0) \sin 2\theta_s(0) \rangle} \tag{III.8a}$$

$$S_{1s}(\omega) = \mathrm{FFT}[S_{1s}(t)] \quad S_{1s}(t) = \frac{\langle \sin \theta_s(t) \sin \theta_s(0) \rangle}{\langle \sin \theta_s(0) \sin \theta_s(0) \rangle} \tag{III.8b}$$

$S_{2s}(\omega)$ and $S_{1s}(\omega)$ are shown on Figures 8 and 9 where they appear indeed to be quite similar to the spectral densities $S_2(\omega)$ and $S_1(\omega)$. These correlations functions reflect two aspects of the pseudo spin dynamics: first, the finite residence time of the dumbbells in a given potential well which is often referred to as the lifetime of librations and second the effective reorientational motions from one potential well to another. The duration of an effective reorientation is also finite (for a temperature of 300 K, the mean velocity of a free rotation of a dumbbell $\sqrt{kT/I}$ is

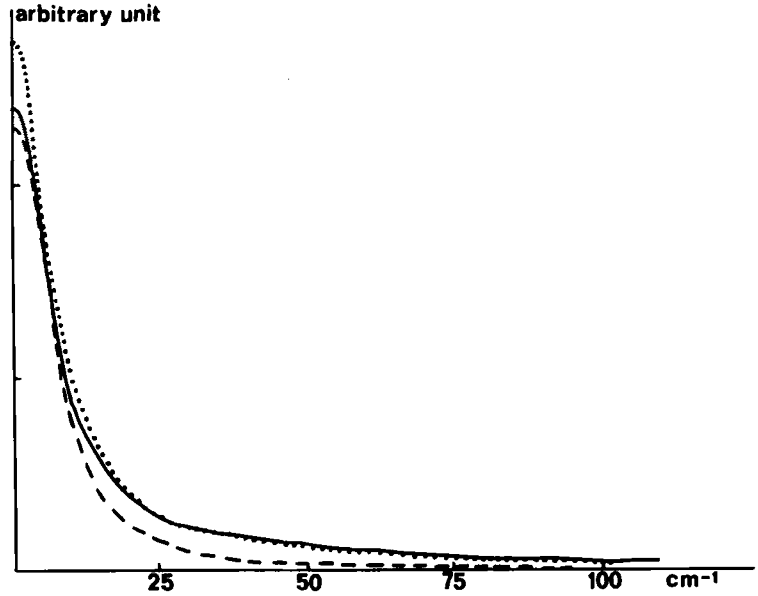

FIGURE 8 Comparison between three different spectral density functions.
a) *full line*: spectral density $S_{2s}(\omega)$ of the pseudospin correlation function

$$\frac{\langle \sin 2\theta_s(t) \sin 2\theta_s(0)\rangle}{\langle \sin 2\theta_s(0) \sin 2\theta_s(0)\rangle}$$

b) *broken line*: spectral density $F_2(\omega)$ of the fitted exponential correlation function

$$\lambda_2\, e^{-t/\tau_2}$$

c) *dotted line*: spectral density $S_2(\omega)$ of the rotational correlation function

$$\frac{\langle \sin 2\theta(t) \sin 2\theta(0)\rangle}{\langle \sin 2\theta(0) \sin 2\theta(0)\rangle}$$

about 7.4 10^{+12} rd/s which corresponds to 0.4 ps for a free rotation of an angle π). However if we analyze the dynamics with a poor resolution time (e.g. $\Delta t \geqslant 0.64$ ps), the reorientations can appear as instantaneous jumps and we can analyze the correlation functions $S_{2s}(t)$ and $S_{1s}(t)$ (for $t \geqslant \Delta t$) in the framework of the theory developed by Rigny.[23] In this framework, we assume that the possible reorientations of the dumbbells belong to the C_4 rotational group. Then, as each test function $\sin 2\theta_s$ and $\sin \theta_s$ belongs to a different irreducible representation of the group C_4, $S_{1s}(t)$ and $S_{2s}(t)$ must have an exponential behavior with different relaxation times: τ_1 and τ_2

$$S_{1s}(t) = \lambda_1\, e^{-t/\tau_1} \qquad \text{(III.9a)}$$

$$S_{2s}(t) = \lambda_2\, e^{-t/\tau_2} \qquad \text{(III.9b)}$$

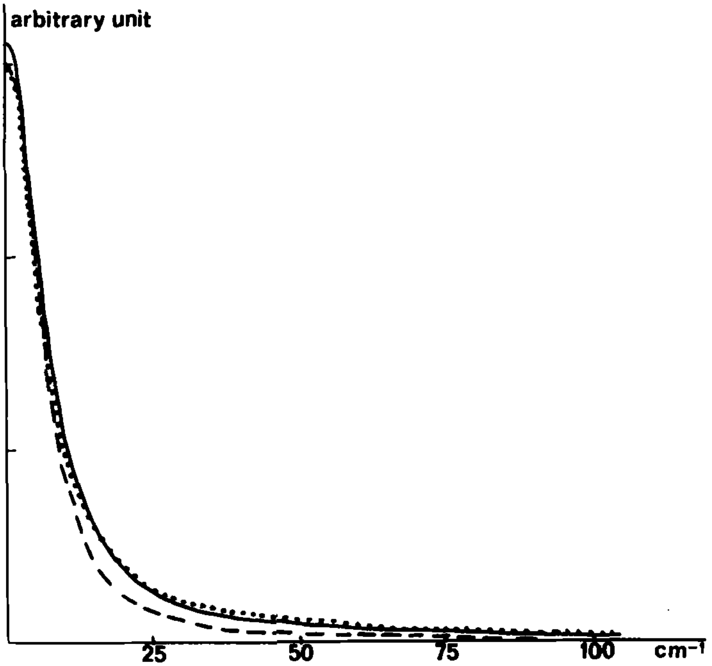

FIGURE 9 Comparison between three different spectral density functions.
a) *full line*: spectral density $S_{2s}(\omega)$ of the pseudospin correlation function

$$\frac{\langle \sin\theta_s(t)\sin\theta_s(0)\rangle}{\langle \sin\theta_s(0)\sin\theta_s(0)\rangle}$$

b) *broken line*: spectral density of the fitted exponential correlation function

$$\lambda_1 e^{-t/\tau_1}$$

c) *dotted line*: spectral density of the rotational correlation function

$$\frac{\langle \sin\theta(t)\sin\theta(0)\rangle}{\langle \sin\theta(0)\sin\theta(0)\rangle}$$

The formulae (III.9) were used in a least square fit of the computed correlations $S_{1s}(t)$ and $S_{2s}(t)$ for $t > 0.64$ ps. This fit gives the following results

$$\lambda_1 \approx 0.7, \quad \lambda_2 \approx 0.6 \tag{III.10}$$

and

$$\tau_1 = \tau_2 = 1 \pm 0.1 \text{ pcs}$$

These results imply that the probability of a C_4^1 jump (reorientation of an angle $\pi/2$) which is a change from one of the two preferred orientations to the other is nearly equal to the probability of a C_4^2 jump (reorientation of an angle π) which implies that, after the reorientation the dumbbell find again the same potential well. This fact which may seem surprising at first sight is in fact easily understood if we recall that orientational motions do not occur as thermally activated jumps over a fixed potential barrier. More likely, a dumbbell goes into reorientational motion when a favorable conjunction of the translational modes relaxes for a while the surrounding cage of A^+ atoms. Then, the dumbbell can rotate nearly freely before being trapped in a new potential well which has little statistic correlation with the initial one and can be, with almost equal probability, in one of the two preferred directions. At last, we can derive from this analysis a more important result which is an evaluation of the average residence time, τ, (or librational lifetime) of the dumbbell in a given potential well. Following the analysis of Rigney *et al.*[23] one obtains easily:

$$\tau = \frac{4\ \tau_1 \times \tau_2}{2\ \tau_2 + \tau_1} \simeq 1.25 \text{ pcs} \qquad \text{(III.11)}$$

As the mean librational frequency is about 120 cm^{-1} (see next section), the above result means that, in average a librational interval is lasting for about five oscillations.

Although for technical numerical reasons, the relaxation times τ_1 and τ_2 were deduced from a fit of the time correlation functions, we have drawn on Figures 8 and 9, the corresponding spectral density

$$F_1(\omega) = \text{FFT}(\lambda_1\ e^{-t/\tau_1}) \qquad \text{(III.12a)}$$

and

$$F_2(\omega) = \text{FFT}(\lambda_2\ e^{-t/\tau_2}) \qquad \text{(III.12b)}$$

Apart from the elastic ($\omega = 0$) limit, these spectral densities fit the pseudo spin spectral densities $S_{2,s}(\omega)$ and $S_{2,s}(\omega)$ in the low frequency part of the spectra. Of course the difference between the high frequency tails of $F_1(\omega)$ and $S_{1,s}(\omega)$ [respective of $F_2(\omega)$ and $S_2(\omega)$] arises from the intervals of effective reorientations of the dumbbells.

d) The inhomogeneous broadening of the librational spectra. The lineshape of $C_2(\omega)$ is not purely librational since, at least, it can be seen from Eq. III.7 that this spectrum involves a convolution product with the spectral density of a pseudo spin function. However, in view of the above result, this convolution product cannot account for the 150 cm^{-1} width of $C_2(\omega)$. Following ideas currently admitted in the study of liquid states, the anomalous width of librational spectra is sometimes attributed to the short lifetime of librational intervals. This explanation neither fits our simulated system where the lifetime of librations is about 1.25 ps (which implies a spectral width $\Delta\omega$ of only 5 cm^{-1}) nor the experimental fact that the librational linewidth of the F_{2g} Raman spectrum of NaCN [which is the 3*d* analogue of $C_2(\omega)$] is nearly independent of the temperature over the whole temperature range of the plastic phase.[13] This last experimental fact implies moreover that the anharmonicity of the librational motion does not play a very important role; we are led to think that the major part of the librational linewidth arises in fact from a dispersion of the librational frequencies due to the spatial inhomogeneity of the crystal at a given time. This "inhomogeneous broadening" arises from the quasi static structural disorder of the ODIC phase: at a given time each dumbbell has a different surrounding cage and thus feels a different rotational potential. To check this hypothesis, we computed an estimate of the importance of the inhomogeneous broadening in the following way: for a few configurations of the sample obtained in the course of the molecular dynamics run, we assumed that the centers of mass of the A^+ ions were suddenly frozen in their actual positions. For each dumbbell we computed the best translational and orientational position by a minimization of the repulsive potential arising from the surrounding frozen cage of A^+ atom. The second derivative of this potential with respect to the angular coordinate of the dumbbell was then taken as an estimate of a librational frequency. The obtained frequencies are displayed as an histogram on Figure 10. This histogram shows a large distribution of frequencies extending roughly from 50 cm^{-1} up to 200 cm^{-1}; the first moment of this histogram which can be considered as the mean librational frequency is about 120 cm^{-1}.

The comparison between Figures 7 and 10 is rather striking and shows that, indeed the major part of the linewidth of Figure 7 comes from this inhomogeneous linewidth. In the calculation leading to Figure 10 a possible coupling of the librational modes with translational one is completely neglected. Thus the good agreement between Figures 7 and 10 implies also that such a coupling plays no important role in our system. In fact, despite the strong relation between reorientational motions and translational modes, the bottom well librational excitations seemed to be quite independent from the other dynamical processes (translations and reorientations). This fact which is usually assumed in the various study of plastic phases appears clearly on the dispersion curves of the low temperature phase (Figure 2) where the percentage of the librational character in a given mode is shown for the different branches at various points of the reciprocal space. Such a

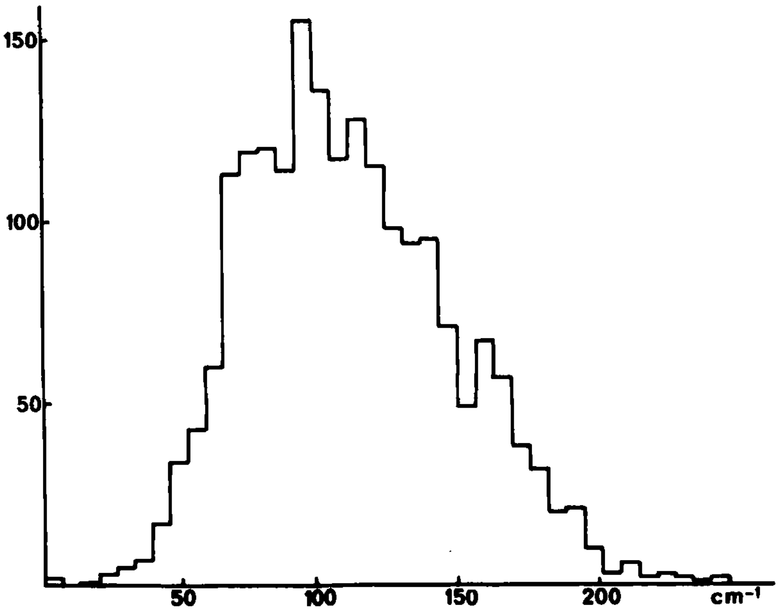

FIGURE 10 Histogram of the harmonic librational frequencies. Compare with Figure 6.

study was already made by Windsor *et al.*[24] in the case of adamantane and led to a similar result.

CONCLUSION

The molecular dynamics calculation presented here is the first step of a systematic study of ODIC phases through computer simulations. In this paper, we have confined ourselves to a limited number of points, studying a $2d$ model the characteristics of which were, in many respects, designed to be reminiscent of those of the plastic phase of an alkali cyanide (NaCN for instance). The main points which have come out of this study are the following:

1) At a given time, the local structure of the ODIC phase is very similar to that of the low temperature phase of our model.

2) The probability distribution function $P(\theta)$ has the square symmetry of the mean ODIC lattice, with maxima along $[1, 1]$ and $[1, \bar{1}]$ directions.

3) The reorientational dynamics of the dumbbells can be analyzed through the study of some appropriate self-correlation functions, such as those of $\sin \theta(t)$ or $\sin 2\theta(t)$. The analysis shows that the notion of a time of residence at the bottom of a potential well, τ_R, is meaningful in our case ($\tau_R \simeq 1.2$ pcs) and that the probability for making 90° and 180° reorientations are approximately equal. The exponential decay related to such a probability is the prominent feature of the corresponding spectra, and appears as a very intense and narrow central peak. The high frequency part of these spectra contain the informations related to the finite duration of the reorientation processes; nevertheless we have not yet been able to obtain a reliable enough numerical accuracy to properly analyze those effects which are clearly visible in our calculations.

4) The librations of the dumbbells near the bottom of their potential well can be rather properly isolated in the self-correlation function of $\cos 2\theta(t)$. These librations appear as a very broad band, centered around 120 cm^{-1}, with a HWHM of ~50 cm^{-1}. Our analysis shows that this band width is completely dominated by the inhomogeneous broadening due to the various orientational potentials experienced by the different dumbbells; on the contrary the finite lifetime of the librations and the orientational–translational coupling play here a very minor role.

All these results agree well with our present knowledge of plastic phases. They also emphasize the necessity of measuring different correlation functions, on a wide frequency range in order to properly analyze the orientational dynamics of such phases. For instance in NaCN, the librational spectrum is attained through the function $\{-(1/\sqrt{2})[Y_2^1(\theta,\varphi) - Y_2^{-1}(\theta,\varphi)]\}$ and the reorientational dynamics through $Y_2^0(\theta,\varphi)$. Nevertheless up to now, the latter has not been measured at low enough frequency to directly extract the residence time out of it.

It is also important to note that our analysis has been performed at one given temperature (300 K), close to the order–disorder transition of the system and for one value of the moment of inertia of the dumbbell.

- An increase of T will certainly decrease the ratio between the time of residence, τ_R, and the mean period of libration of the dumbbell. In the present calculation, this ratio is approximately 5, and it will be important to see if it remains large enough close to the melting temperature, to allow for the notion of well-defined librations to persist over the whole ODIC phase.

- Though no spatial (static or dynamical) correlation functions have been computed in this paper, a direct look at drawings, such as those of Figure 2, taken at different times, shows that the reorientational dynamics involves essentially local effects. This is primarily due to our choice of parameters so that the librational frequencies of the low temperature phase, some zone boundary phonons and the free rotation frequency of the dumbbells are roughly equal. In such a case (which is the situation for the alkali cyanides) a time typical for a reorientation process, matches with that of a local fluctuation of the position of the four nearest neighbors of a given dumbbell. This matching will not survive if the moment of inertia increases; the mechanism allowing for the reorientational processes in this latter case will need to be carefully analyzed through the spatial correlation functions. This will be the subject of a forthcoming paper.

References

1. *The Plastically Crystalline State*, J. N. Sherwood ed., (Wiley and Sons, New York, 1979).
2. *Vibrational Spectroscopy of Molecular Liquids and Solids*, S. Bratos and R. M. Pick eds. (Plenum Press, New York, 1980).
3. K. H. Michel and H. de Raedt, *J. Chem. Phys.*, **65**, 977 (1976).
4. K. H. Michel and J. Naudts, *J. Chem. Phys.*, **67**, 547 (1977).
5. K. H. Michel and J. Naudts, *J. Chem. Phys.*, **68**, 216 (1978).
6. H. J. Verweel and J. N. Bijvoet, *Z. Krist.*, **100**, 201 (1938).
7. D. L. Price, J. M. Rowe, J. J. Rush, E. Prince, D. G. Hinks and S. Susman, *J. Chem. Phys.*, **56**, 3697 (1972).
8. J. M. Rowe, D. G. Hinks, D. L. Price, S. Susman and J. J. Rush, *J. Chem. Phys.*, **58**, 2039 (1973).
9. D. Fontaine, R. M. Pick and M. Yvinec, *Solid State Commun.*, **21**, 1095 (1977).
10. S. Haussuhl, J. Eckstein, K. Recker and F. Wallrafen, *Acta Cryst.*, **A33**, 847 (1977).
11. M. Boissier, R. Vacher, D. Fontaine and R. M. Pick, *J. Physique*, **41**, 1437 (1980).
12. J. J. Rush, J. M. Rowe, N. Vagelatos, D. L. Price, D. G. Hinks and S. Susman, *J. Chem. Phys.*, **62**, 4551 (1975).
13. D. Fontaine and R. M. Pick, *J. de Physique*, **40**, 1105 (1979).
14. M. L. Klein and I. R. McDonald, *Chem. Phys. Lett.*, **78**, 383 (1981).
15. M. Born and K. Huang, *Dynamical Theory of Crystal Lattice*, Clarendon Press, Oxford, p. 26 (1968).
16. M. Parrinello and A. Rahman, *Phys. Rev. Letters*, **45**, 1196 (1980).
17. W. Press, *J. Chem. Phys.*, **56**, 2597 (1972).
18. L. Verlet, *Phys. Rev.*, **159**, 98 (1967).
19. S. G. Brush, H. L. Sahlin and E. Teller, *J. Chem. Phys.*, **45**, 2102 (1966).
20. K. E. Larsson, *J. Chem. Phys.*, **59**, 4612 (1973).
21. J. L. Sauvajol *et al.*, to be published.
22. M. Yvinec and R. M. Pick, *J. de Physique*, **41**, 1045 (1980). R. M. Pick and M. Yvinec, *J. de Physique*, **41**, 1053 (1980).
23. P. Rigny, *Physica*, **59**, 707 (1973). C. Thibaudier and F. Volino, *Molecular Physics*, **26**, 1281 (1973).
24. C. G. Windsor, D. H. Saunderson, J. N. Sherwood, D. Taylor and G. S. Pawley, *J. Phys. C*, **11**, 1741 (1978).